[4] D. W. Morel, J. R. Hessler, G. M. Chisolm, *J. Lipid Res.* **1983**, *24*, 1070–1076.
[5] U. P. Steinbrecher, S. Parthasarathy, D. S. Leake, J. L. Witztum, D. Steinberg, *Proc. Natl. Acad. Sci. USA.* **1984**, *81*, 3883–3887.
[6] U. P. Steinbrecher, H. Zhang, M. Lougheed, *Free Radicals Biol. Med.* **1990**, *9,* 155–168.
[7] J. A. Berliner, M. C. Territo, A. Sevanian, R. Soroush, J. A. Kim, B. Bamshad, M. Esterson, A. M.Fogelman, *J. Clin. Invest.* **1990**, *85*, 1260–1266.
[8] H. Esterbauer, G. Jürgens, O. Quehenberger, E. Koller, *J. Lipid Res.* **1987**, *28*, 495–509.
[9] F. J. G. M. van Kuijk, A. N. Siakotos, L. G. Fong, R. J. Stephens, D. W. Thomas, *Anal. Biochem.* **1995**, *224*, 420–424.
[10] T. Wang, W. G. Yu, W. S. Powell, *J. Lipid Res.* **1992**, *33*, 525–537.
[11] H. W. Gardner, R. Kleiman, D. Weisleder, *Lipids* **1974**, *9*, 696–706.
[12] E. N. Frankel, *J. Am. Oil Chem. Soc.* **1984**, *61*, 1908–1917.
[13] C. Schwarz and G. Spiteller, unpublished results.
[14] W. Jira, G. Spiteller, W. Carson, A. Schramm, *Chem. Phys. Lipids* **1998**, *91*, 1–11.
[15] H. Esterbauer, R. J. Schaur, H. Zollner, *Free Radicals Biol. Med.* **1991**, *11*, 81–128.
[16] H. Esterbauer, J. Gebicki, H. Puhl, G. Jürgens, *Free Radicals Biol. Med.* **1992**, *13*, 341–390.
[17] C. E. Thomas, R. L. Jackson, D. F. Ohlweiler, G. Ku, *J. Lipid Res.* **1994**, *35*, 417–427.
[18] L. Nagy, P. Tontonoz, J. G. Alvarez, H. Chen, R. M. Evans, *Cell* **1998**, *93*, 229–240.
[19] A. Chawla, E. J. Schwarz, D. D. Dimaculangan, *Endocrinology* **1994**, *135*, 798–800.
[20] D. Moch, T. Schewe, H. Kuehn, D. Schmidt, P. Buntrock, *Biomed. Biochim. Acta* **1990**, *49*, 201–207.
[21] G. A. Blondin, *Ann. N. Y. Acad. Sci. (Carriers Channels Biol. Syst.)* **1975**, *264*, 98–111.
[22] K. Uchida, S. Toyokuni, K. Nishikawa, S. Kawakishi, H. Oda, H. Hiai, E. R. Stadtman, *Biochemistry* **1994**, *33*, 12487–12494
[23] S. Srivastava, A. Chandra, L.-F. Wang, W. E. Seifert, Jr., B. B. DaGue, N. H. Ansari, S. K. Srivastava, A. Bhatnagar, *J. Biol. Chem.* **1998**, *273*, 10893–10900.
[24] T. Kaneko, S. Honda, S. I. Nakano, M. Matsuo, *Chem. Biol. Interact.* **1987**, *63*, 127–137.
[25] D. Steinberg, *Atherosclerosis Reviews 18* (Eds.: J. Stokes, M. Mancini), Raven, New York, **1988**, 1–23.
[26] D. Steinberg, *J. Biol. Chem.* **1997**, *272*, 20963–20966.
[27] W. Jira, G. Spiteller, A. Schramm, *Chem. Phys. Lipids* **1996**, *84*, 165–173.
[28] O. Leiss, U. Murawski, H. Egge, *J. Clin. Chem. Clin. Biochem.* **1979**, *17*, 619–625.
[29] E. G. Bligh, W. J. Dyer, *Can. J. Biochem. Physiol.* **1959**, *37*, 911–917.
[30] P. Spiteller, G. Spiteller, *Chem. Phys. Lipids* **1997**, *89*, 131–139.
[31] P. Spiteller, G. Spiteller, *Biochim. Biophys. Acta* **1998**, *1392*, 23–40.

Radical Intermediates in the Jacobsen–Katsuki Epoxidation[**]

Luigi Cavallo and Heiko Jacobsen[*]

The generation of optically active epoxides by oxygen-transfer reactions represents one of the most elegant techniques used in the formation of carbon–oxygen bonds in asymmetric synthesis.[1] The catalytic protocol developed by Jacobsen and co-workers,[2] which involves the use of the Mn^{III}–salen complex **1** and derivatives thereof, currently stands as the most powerful method in this field; it has been proven effective for virtually every class of unfunctionalized, conjugated olefins,[3] and industrial production of the catalyst on a ton scale has become possible.[4] Although the importance of steric bulk in the 3,3′-position of the salen ligand and the profound influence of electronic effects due to the substituents in 5,5′-position were recognized early on[5] and rationalized in model calculations,[6] the mechanism of the Mn^{III}–salen catalyzed epoxidation is still a matter of controversy. The *cis–trans* isomerization observed in the transformation of conjugated alkenes gave rise to several proposed mechanisms. Starting with a Mn^{V}-oxo-salen complex as the catalytically active species—experimental evidence has recently been provided for this[7]—the reaction might proceed either by direct substrate attack at the oxo ligand in a concerted or sequential fashion involving radical intermediates, or by substrate attack at both the metal and oxo centers to generate an oxametallacyclic intermediate (Scheme 1, pathways **Ic**, **Is**, and **II**, respectively). New experimental results seem to provide evidence for substrate attack at the oxo ligand only,[8] as well as for the existence of manganaoxetanes;[9] the controversial mechanistic debate has recently been summarized in a highlight.[10]

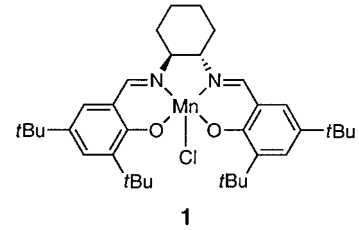

1

---

[*] Dr. H. Jacobsen
Anorganisch-Chemisches Institut
Unversität Zürich
Winterthurerstrasse 190, 8057 Zürich (Switzerland)
Fax: (+41) 1-635-6802
E-mail: jacobsen@aci.unizh.ch

Dr. L. Cavallo
Dipartimento di Chimica
Università degli Studi di Napoli “Federico II”
Via Mezzocannone 4, 80134 Napoli (Italy)

[**] L.C. acknowledges financial assistance from the Ministero della Ricerca Scientifica e Tecnologica. H.J. is indebted to Prof. H. Berke for continued support.

Supporting information for this article is available on the WWW under http://www.wiley-vch.de/home/angewandte/ or from the author.

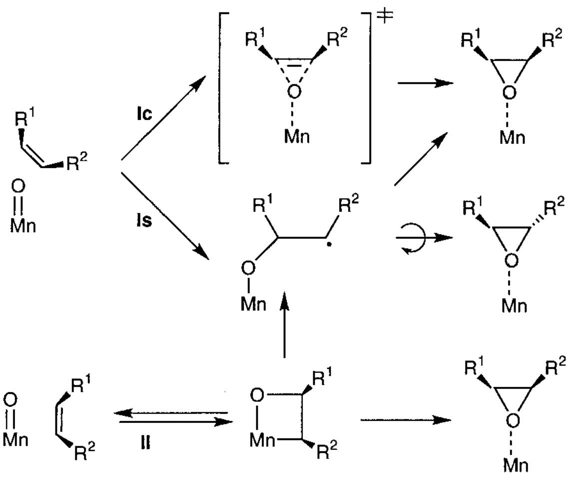

Scheme 1. Possible mechanisms for oxygen transfer in the Jacobsen–Katsuki epoxidation. For **Is**, rotational collapse leads to the *trans* epoxide, whereas direct collapse leads to the same *cis* product as pathway **Ic**.

Given the importance of the Jacobsen–Katsuki epoxidation, we decided to examine its mechanism in a quantum chemical study based on density functional theory.[11, 12] The starting point of our calculations was the Mn^{III} model complex **2** and its oxo derivative **3** (Figure 1). In both cases, we considered triplet and quintet configurations corresponding to a value for the total spin density of 2α, *S*2, and 4α, *S*4, respectively. For **2**, the *S*2 geometry lies 38 kJ mol^{-1} above the *S*4 ground state in energy. Also, for the *S*4 geometry of **2**, characteristic parameters such as the Mn–Cl and Mn–N distances are in close agreement with the values obtained from a crystal structure analysis of **1**.[13] For **3**, we found that an *S*2 ground state is favored over an *S*4 geometry by 45 kJ mol^{-1}. Thus, the first step in the catalytic cycle, which is also the rate-determining step,[8] requires a change of the electronic configuration at the metal center. The mechanistic details of the oxidation reaction are, however, beyond the scope of the present work, and will not be discussed further. Instead, we will focus on the sequence of steps needed in C–O bond formation.

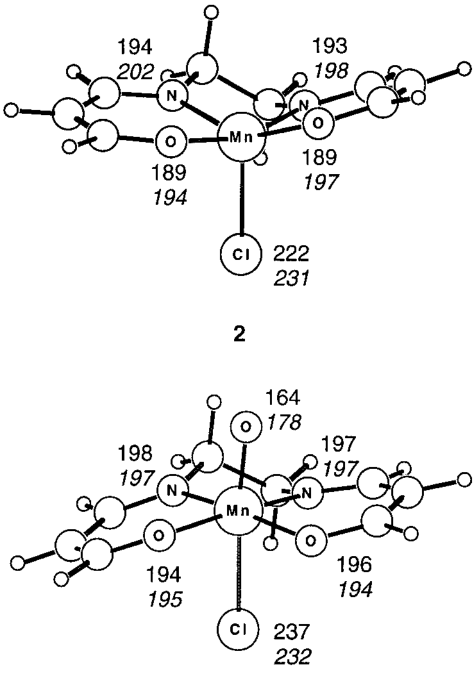

2

3

Figure 1. Geometries for **2** and **3** optimized on the *S*2 and *S*4 surface (Calculations on the BP86 level; *S*4 values in italics). Experimental bond lengths [pm][13] for **1**: Mn-Cl: 236.0; Mn-N: 200.3, 195.7; Mn-O: 184.8, 187.2.

The *S*2 energy profiles for the epoxidation reaction along pathways **Is** and **Ic** are displayed in Figure 2a. The reference state at 0 kJ mol^{-1} is system **4**, in which the olefin enters the coordination sphere of **3**, about 280 pm from the oxo center. Along pathway **Is**, the formation of the radical intermediate **6** (Figure 3) passes through the transition state $5^{\ddagger}$, with O–$C_{C_2H_4}$ distances of 201 and 267 pm. The activation energy for this step amounts to only 12 kJ mol^{-1}. The radical intermediate **6** is 40 kJ mol^{-1} more stable in energy than **4**. It possesses a spin density of approximately 3α at the Mn center and 1β at the terminal C atom of the olefin ligand, indicating that a one-electron reduction process has taken place. The radical **6** can collapse directly with almost no energy barrier via $7^{\ddagger}$ to yield

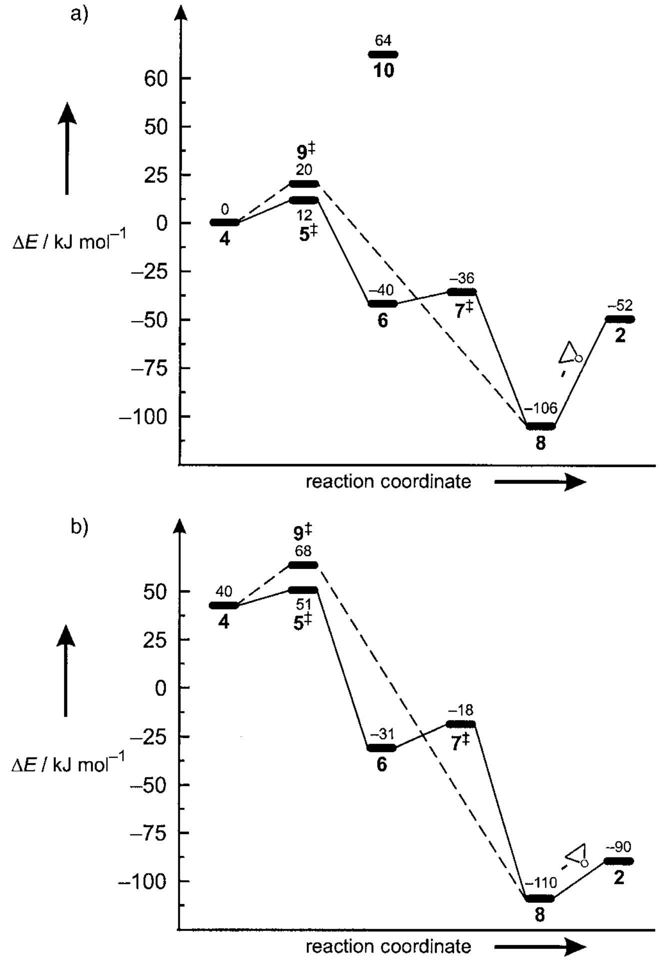

Figure 2. Energy profiles for the epoxidation reaction on a) the *S*2 and b) the *S*4 surface.[16] Solid lines refer to pathway **Is**, broken lines to **Ic**.

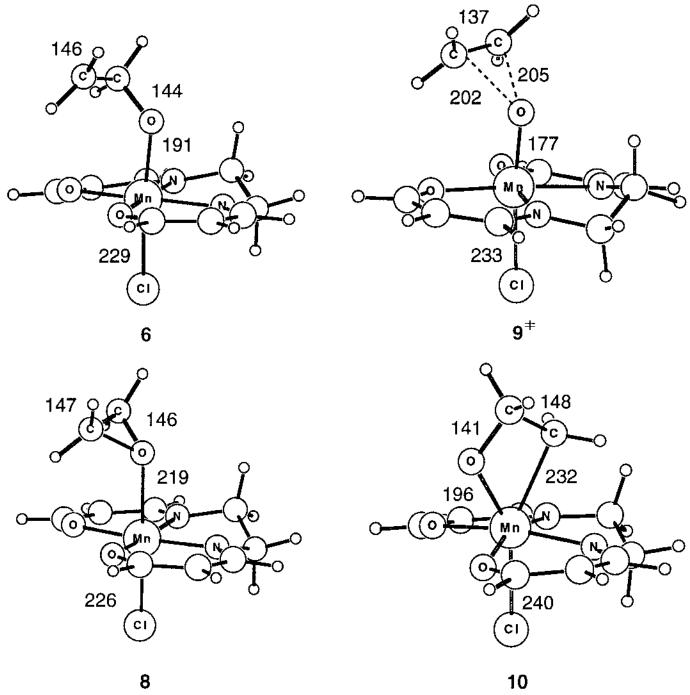

Figure 3. Geometries for key structures in the *S*2 epoxidation reaction (Calculations on the BP86 level; all distances in pm).

the epoxide complex **8** (Figure 3), which lies 106 kJ mol^{-1} below **4**. The rotational route, instead, requires a torsion around the sp^2-sp^3 C–C bond in **6** prior to product formation. A barrier of 10 kJ mol^{-1} is calculated for this process.

Hence, when comparing rotational collapse with direct collapse, the latter represents the path of lower activation barrier, even for the sterically unencumbered model olefin examined here. This finding is in qualitative agreement with the experimentally observed limited conversion of *cis* olefins such as *cis*-β-methylstyrene into the thermodynamically more stable *trans* epoxide.[8] The epoxide detachment from **8** eventually regenerates the Mn^{III} species **2** in a step which requires 54 kJ mol^{-1}. However, taking into account the unfavorable coordination entropy, product liberation is not a critical step in the catalytic cycle.[14]

The alternative pathway **Ic** branches at **4**, and proceeds via transition state $\mathbf{9}^{\ddagger}$ (Figure 3). This path, which corresponds to a simultaneous attack of both alkene C atoms at the oxo center, requires an activation energy of 20 kJ mol^{-1}. For $\mathbf{9}^{\ddagger}$ we find a value of roughly 2α for the spin density at the metal center, which shows that the final bond-forming step will occur as a two-electron reduction process.

The reaction sequences **Is** and **Ic** have also been investigated on the *S*4 energy surface, and the energy profiles are displayed in Figure 2b. For comparison, *S*2-**4** was again taken as the reference system at 0 kJ mol^{-1}. In all cases directly involved in product formation, the *S*2 geometries are lower in energy, with the exception of **8**, for which the *S*4 state is a mere 4 kJ mol^{-1} more stable. This leads to the conclusion that the formation of the epoxide occurs under conservation of spin.

If the spectator position *trans* to the oxo function is always occupied during the catalytic cycle, the oxametallacycle formed according to reaction pathway **II** requires a seven-coordinated ligand environment at the manganese center. The manganaoxetane **10** (Figure 3) lies 64 kJ mol^{-1} higher in energy than **4**, and even 104 kJ mol^{-1} above **6**, and does not represent a feasible entry into the epoxidation route. A six-coordinate manganaoxetane intermediate might be realized if predissociation of the spectator ligand takes place,[15] but experimental evidence strongly suggests that in the active catalyst no free coordination site is available.[8]

We further performed full geometry optimizations for structures **3** and **6**, in which a salen ligand was used in place of the simpler model ligand considered so far.[16] With the salen ligand, the *S*2 states for **3** and **6** were calculated to be more stable than the *S*4 states by 46 and 9 kJ mol^{-1}, respectively, which is virtually identical to the values of 45 and 9 kJ mol^{-1}, obtained with the simpler model ligand. Compared to the free species, the radical intermediates *S*2-**6** and *S*4-**6** with the salen ligand are more stable in energy by 39 and 75 kJ mol^{-1}; again in close agreement to the values of 38 and 74 kJ mol^{-1} obtained for the simplified system. These and similar results obtained for related Co compounds[17] indicate that within the chosen computational approach, the Mn complexes employed here are appropriate models for the description of the main changes in electronic structure which occur during the epoxidation process.

In summary, the Jacobsen–Katsuki epoxidation occurs by direct attack of the olefin at the oxo ligand of the Mn–salen catalyst, and is likely to involve radical intermediates (pathway **Is**, Scheme 1). The reaction proceeds on the *S*2-energy surface.[18] The relative stability of the radical intermediate and the relative height of the activation barriers for collapse and rotation determine the amount of *cis*–*trans* isomerization in the final epoxidation product. In systems which seem to follow reaction path **Ic**, a possible radical intermediate would have a very short lifetime and collapses with almost no activation barrier. A pathway **II** via an oxametallacycle can be excluded for energy reasons, and the formation of a manganaoxetane is disfavored compared to the radical route, even if a free coordination site is available.[15]

Received: April 12, 1999
Revised: August 11, 1999[Z13271]

---

[1] a) E. N. Jacobsen in *Catalytic Asymmetric Synthesis* (Ed.: I. Ojima), VCH, Weinheim, **1993**, chap. 4.2; b) E. N. Jacobsen in *Comprehensive Organometallic Chemistry II, Vol. 12* (Eds.: G. Wilkinson, F. G. A. Stone, E. W. Abel, L. S. Hegedus), Pergamon, New York, **1995**, chap. 11.1.

[2] a) W. Zhang, J. L. Loebach, S. R. Wilson, E. N. Jacobsen, *J. Am. Chem. Soc.* **1990**, *112*, 2801; b) E. N. Jacobsen, W. Zhang, M. L. Güler, *J. Am. Chem. Soc.* **1991**, *113*, 6703; c) E. N. Jacobsen, W. Zhang, A. R. Muci, J. R. Ecker, L. Deng, *J. Am. Chem. Soc.* **1991**, *113*, 7063.

[3] T. Katsuki, *Coord. Chem. Rev.* **1995**, *140*, 189.

[4] J. F. Larrow, E. N. Jacobsen, Y. Gao, Y. Hong, X. Nie, X. M. Zepp, *J. Org. Chem.* **1994**, *59*, 1939.

[5] M. Palucki, N. S. Finney, P. J. Pospisil, M. L. Güler, T. Ishida, E. N. Jacobsen, *J. Am. Chem. Soc.* **1998**, *120*, 948.

[6] P.-O. Norrby, C. Linde, B. Åkermark, *J. Am. Chem. Soc.* **1995**, *117*, 11035.

[7] D. Feichinger, D. A. Plattner, *Angew. Chem.* **1997**, *109*, 1796; *Angew. Chem. Int. Ed. Engl.* **1997**, *36*, 1718.

[8] N. S. Finnley, P. J. Pospisil, S. Chang, M. Palucki, R. G. Konsler, K. B. Hansen, E. N. Jacobsen, *Angew. Chem.* **1997**, *109*, 1798; *Angew. Chem. Int. Ed. Engl.* **1997**, *36*, 1720.

[9] C. Linde, M. Arnold, P.-O. Norrby, B. Åkermark, *Angew. Chem.* **1997**, *109*, 1802; *Angew. Chem. Int. Ed. Engl.* **1997**, *36*, 1723.

[10] T. Linker, *Angew. Chem.* **1997**, *109*, 2150; *Angew. Chem. Int. Ed. Engl.* **1997**, *36*, 2060.

[11] The self-consistent GGA-BP86 calculations were performed using the ADF program package, version 2.3.[12] Main group elements were described by a double ζ STO basis including one polarization function, whereas for Mn a triple ζ STO basis with one additional 4p function was used (ADF basis sets III and IV, respectively). Transition states have been characterized by one negative eigenvalue of the approximate Hessian, and by a coordinate-tracing procedure. For more computational details and further references, see ref. [12d].

[12] a) E. J. Baerends, D. E. Ellis, P. E. Ros, *Chem. Phys.* **1973**, *2*, 41; b) G. teVelde, E. J. Baerends, *J. Comp. Phys.* **1992**, *99*, 84; c) C. Fonseca-Guerra, O. Visser, J. G. Snijders, G. teVelde, E. J. Baerends in *Methods and Techniques in Computational Chemistry: METECC-95* (Eds.: E. Clementi, G. Corongiu) STEF, Cagliari, **1995**, p. 305; d) G. teVelde, *ADF 2.3 User's Guide,* Vrije Universiteit, Amsterdam, **1997**.

[13] P. J. Pospisil, D. H. Carsten, E. N. Jacobsen, *Chem. Eur. J.* **1996**, *2*, 974.

[14] Experimental data (F. C. Rix, M. Brookhart, P. S. White, *J. Am. Chem. Soc.* **1996**, *118*, 4746), and theoretical calculations (D. G. Musaev, R. D. J. Froese, M. Svensson, K. Morokuma, *J. Am. Chem. Soc.* **1997**, *119*, 367; P. Margl, L. Deng, T. Ziegler, *Organometallics* **1998**, *17*, 933) suggest that at room temperature the $-T\Delta S$ contribution to the free energy of ethene coordination to transition metal d^0 and d^8 compounds is in the range 40–50 kJ mol^{-1}. It is argued that enthalpies of coordination higher than 50 kJ mol^{-1} are needed to give rise to stable ethene-coordinated species. A similar $-T\Delta S$ contribution to the free energy of epoxide coordination, and hence similar conclusions, can also be reasonably assumed in the present study.

[15] C. Linde, B. Åkermark, P.-O. Norrby, M. Svensson, *J. Am. Chem. Soc.* **1999**, *121*, 5083.

[16] Consult the supporting information for optimized geometries and final energies of all species.

[17] N. J. Henson, P. J. Hay, A. Redondo, *Inorg. Chem.* **1999**, *38*, 1618.

[18] For **3** and **4**, besides the *S*2 and *S*4 cases already discussed, we also located singlet *S*0 geometries, within 3 kJ mol^{-1} of the related triplet species. The formation of *S*0-**6** and *S*0-**9**$^+$ from *S*0-**4** is, however, endothermic by 33 and 91 kJ mol^{-1}, respectively. Thus, the epoxide formation is not likely to occur on the *S*0 surface. For a discussion of the different spin states of Mn^{V}–oxo complexes, see also ref. [15]. For **2** and **10**, no complexes possessing *S*0-ground states could be localized.

Molecular Design of Liquid-Crystalline Block Molecules: Semifluorinated Pentaerythritol Tetrabenzoates Exhibiting Lamellar, Columnar, and Cubic Mesophases**

Xiao Hong Cheng, Siegmar Diele, and Carsten Tschierske*

The spontaneous formation of fluid supermolecular assemblies with well-defined morphologies (e.g. layers, interpenetrating networks, columns, and spheroids) is fundamental for structure formation in biological systems as well as for the tailoring of novel materials. Thus, the investigation of the driving forces of this self assembly process and the rational design of molecules which can form specific supermolecular structures on different length scales are contemporary research topics. Molecules, able to self assemble to these well-organized states of soft matter, can be divided into three classes: anisometric molecules (with a rod- or disclike shape), amphiphilic molecules (lipids/surfactants),[1] and block copolymers.[2] Applications for rodlike thermotropic liquid crystals include electrooptical devices, the lyotropic mesophases of surfactant/water systems can be utilized as templates for the preparation of mesoporous materials, and the ordered structures of block copolymers are, for example, applied in the preparation of ordered arrays of nanosized noble metal and semiconductor particles.

In low molecular weight systems, such as thermotropic liquid crystals, the molecular shape is a major design consideration to tailor the mesophase type. For example, calamitic molecules favor layers (smectic phases), disclike molecules organize to columns (columnar phases), and tapered or cone-shaped amphiphilic[3] or dendritic molecules[4] can form cylindrical or spheroidic aggregates which self assemble into columnar or micellar cubic mesophases. This contrasts with block copolymers, for which no specific molecular shape is necessary to produce a wide range of different morphologies. They can be obtained simply by changing the number and size of the incompatible polymer blocks.[2] The same diversity of different phases can also be found in lyotropic amphiphile/solvent systems with dependence on solvent content and temperature.[1]

The question arose if it would be possible to form different supermolecular structures, previously known from block copolymers and lyotropic systems, with low molecular weight molecules, specifically with molecules built up of different building blocks but without a specific anisometric shape or a pronounced amphiphilicity. Indeed, it was recently shown that star-shaped pentaerythritol tetrakis(3,4-dialkoxybenzoates), such as **2H** (Scheme 1)[5, 6] and related linear compounds,[5b,7]

---

[*] Prof. C. Tschierske, X. H. Cheng
Institut für Organische Chemie der Universität
06120 Halle (Germany)
Fax: (+49) 345-5527030
E-mail: coqfx@mlucom6.urz.uni-halle.de

Dr. S. Diele
Institut für Physikalische Chemie der Universität
06118 Halle (Germany)

[**] This work was supported by the Deutsche Forschungsgemeinschaft and the Fonds der Chemischen Industrie.